CARTER, D. C., RUBLE, J. R. & JEFFREY, G. A. (1982). *Carbohydr. Res.* **102**, 59–67.

GILMORE, C. J. (1983). *MITHRIL. A Computer Program for the Automatic Solution of Crystal Structures from X-ray Data.* Univ. of Glasgow, Scotland.

GOODBY, J. W., MARCUS, M. A., CHIN, E., FINN, P. L. & PFANNEMÜLLER, B. (1988). *Liq. Cryst.* **3**, 1569–1581.

GRAY, G. W. & GOODBY, J. W. (1984). *Smectic Liquid Crystals.* Glasgow, London: Leonard Hill.

HILDRETH, J. E. K. (1982). *Biochem. J.* **207**, 363–366.

JEFFREY, G. A. (1984). *Mol. Cryst. Liq. Cryst.* **110**, 221–237.

JEFFREY, G. A. (1986). *Acc. Chem. Res.* **19**, 168–173.

JEFFREY, G. A. & MALUSZYNSKA, H. (1989). *Acta Cryst.* B45, 447–452.

JEFFREY, G. A. & MITRA, J. (1983). *Acta Cryst.* B39, 469–490.

JEFFREY, G. A., YEON, Y. & ABOLA, J. E. (1987). *Carbohydr. Res.* **169**, 1–11.

KONINGSVELD, H. VAN, JANSEN, J. C. & STRAATHOF, A. J. J. (1988). *Acta Cryst.* C44, 1054–1057.

McPHERSON, A., KOSZELAK, S., AXELROD, H., DAY, J., WILLIAMS, R., ROBINSON, L., McGRATH, M. & CASCIO, D. (1986). *J. Biol. Chem.* **261**, 1969–1975.

MAIN, P., FISKE, S. J., HULL, S. E., LESSINGER, L., GERMAIN, G., DECLERCQ, J.-P. & WOOLFSON, M. M. (1980). *MULTAN80. A System of Computer Programs for the Automatic Solution of Crystal Structures from X-ray Diffraction Data.* Univs. of York, England, and Louvain, Belgium.

MALUSZYNSKA, H. & JEFFREY, G. A. (1987). *Mol. Cryst. Liq. Cryst.* **149**, 1–15.

MOEWS, P. C. & KNOX, J. P. (1976). *J. Am. Chem. Soc.* **98**, 6628–6633.

MÜLLER-FAHRNOW, A., ZABEL, V., STEIFA, M. & HILGENFELD, R. (1986). *J. Chem. Soc. Chem. Commun.* pp. 1573–1574.

PFANNEMÜLLER, B., WELTE, W., CHIN, E. & GOODBY, J. W. (1986). *Liq. Cryst.* **1**, 357–370.

ZABEL, V., MÜLLER-FAHRNOW, A., HILGENFELD, R., SAENGER, W., PFANNEMÜLLER, B., ENKELMANN, V. & WELTE, W. (1986). *Chem. Phys. Lipids*, **39**, 313–325.

The Conformation of Nine-Membered Rings

BY DEBORAH G. EVANS AND JAN C. A. BOEYENS

Department of Chemistry, University of the Witwatersrand, PO Wits, 2050 Johannesburg, South Africa

Abstract

Each of the 16 symmetrical conformations of puckered nine-membered rings is characterized by three amplitude–phase pairs which can be mapped onto the surface of a helical tube that closes into a torus. A projection along the tubular axis, assuming constant radii yields a composite map on which all symmetrical forms can be located unequivocally. The symmetrical forms and representative examples from the literature are analyzed quantitatively in terms of the six primitive forms defined by the three symmetry classes of displacement from a regular planar nonagon.

Introduction

The conformation of an N-membered cyclic compound can be described quantitatively as a linear combination of $N - 3$ primitive forms (Boeyens & Evans, 1989). For small ring systems these are typically the same as the well-known low-energy symmetrical forms, but for large N some of them could present chemically unlikely arrangements (Evans & Boeyens, 1989). As N increases the large number of contributing forms obscures the interpretation of the coefficients in the linear combinations, and for very large rings it is therefore preferable to resort to

different, more intuitive schemes of conformational analysis.

The nine-membered ring is probably the maximum size amenable to analysis by mapping the symmetrical and primitive forms onto an $(N - 3)$-dimensional surface, projected into two for graphical interpretation, a procedure described before for six-, seven- and eight-membered rings by Boeyens (1978), Boessenkool & Boeyens (1980) and Evans & Boeyens (1988), respectively.

Method

The low-energy forms of nine-membered rings and their modes of interconversion were first analyzed by Hendrickson (1964, 1967).

The set of symmetrical conformations need not be limited to the low-energy cycloalkane conformations. Steric factors and crystal-packing forces can force a ring to adopt a conformation other than that of the isolated entity. Sixteen symmetrical conformations, some based on molecular models, have been identified here, including the six conformations detailed by Hendrickson (1964) or postulated as intermediates. These forms are not representative of a particular chemical system, but their bond lengths and angles are within the limits of chemical viability, and

Table 1. Torsion angles (°) and puckering amplitudes (Å) of the classical forms

The symmetry element (C_2 or C_s) passes through the first atom.

Symbol	Symmetry	ω_1	ω_2	ω_3	ω_4	ω_5	q_2	q_3	q_4
BC	C_{3v}	-114	0	114	-114	0	0·00	1·25	0·00
TBC	D_3	-57	130	-57	-57	130	0·00	1·24	0·00
CC	C_s	-69	108	-139	83	0	0·00	0·53	0·87
TCC	C_2	-54	126	-115	80	-77	0·00	0·53	0·87
C	C_s	121	-30	-80	117	0	0·54	1·19	0·22
TC	C_2	-70	100	0	-88	125	0·68	1·04	0·30
B	C_s	-121	39	-80	117	0	1·35	0·39	0·58
TB	C_2	-70	108	-43	72	-143	1·25	0·36	0·53
BB	C_s	67	48	-10	-83	0	2·15	0·00	0·00
TBB	C_2	80	-70	-10	-34	155	2·05	0·00	0·00
CB	C_s	80	-108	0	90	0	1·64	0·67	0·43
TCB	C_2	-72	79	44	-105	93	1·29	0·82	0·45
BC''	C_s	65	51	-140	82	0	0·61	1·09	0·25
TBC''	C_2	-43	124	-88	-28	117	0·64	1·14	0·24
CC''	C_s	-98	72	-134	117	0	0·85	0·40	0·87
TCC''	C_2	-62	120	-84	91	-124	0·90	0·43	0·93

Table 2. Cartesian coordinates of the classical forms

x	y	z	x	y	z
BC			**TBC**		
0·0000	1·5073	0·5937	-0·0000	2·2080	0·0197
1·2671	1·6260	-0·2920	1·2245	1·3889	0·5048
2·0434	0·2833	-0·2960	1·8046	0·3652	-0·5056
1·3088	-0·7595	0·5862	1·9119	-1·0998	-0·0076
0·7709	-1·9181	-0·2937	0·5969	-1·7458	0·5012
-0·7801	-1·9137	-0·2914	-0·5911	-1·7516	-0·4959
-1·3088	-0·7505	0·5878	-1·9087	-1·1071	0·0084
-2·0426	0·2934	-0·2938	-1·8071	0·3616	0·4936
-1·2587	1·6317	-0·2998	-1·2310	1·3806	-0·5213
BC''			**TBC''**		
0·0000	1·9444	-0·6867	-0·0000	2·2052	0·0013
1·3199	1·7364	0·1009	1·2637	1·3869	-0·2239
1·5876	0·2984	0·6167	1·7072	0·0500	0·6222
1·4605	-0·8375	-0·4317	1·9239	-1·1028	-0·3785
0·7848	-2·1452	0·0572	0·5365	-1·7884	-0·5580
-0·7662	-2·1526	0·0596	-0·5362	-1·7888	0·5583
-1·4557	-0·8523	-0·4298	-1·9238	-1·1023	0·3786
-1·5904	0·2844	0·6168	-1·7073	0·0500	-0·6228
-1·3405	1·7241	0·0969	-1·2640	1·3853	0·2228
CC			**TCC**		
0·0000	2·3755	-0·1692	0·0000	1·9299	-0·3678
1·3145	1·6721	0·2585	1·4228	1·7575	-0·0049
1·6138	0·3142	-0·4287	1·7214	0·3581	0·3635
1·4627	-0·9465	0·4619	1·5350	-0·8299	-0·4660
0·7943	-2·1757	-0·2073	0·6506	-1·9882	0·3649
-0·7566	-2·1915	-0·2051	-0·8120	-1·9893	-0·1841
-1·4480	-0·9748	0·4638	-1·7786	-1·0434	0·1800
-1·6271	0·2809	-0·4288	-1·8746	0·3957	-0·3624
-1·3535	1·6458	0·2550	-0·8647	1·4095	0·4680
CC''			**TCC''**		
0·0000	1·8000	0·6200	0·0000	2·1760	0·0000
1·3200	1·6500	-0·2180	1·1200	1·3000	0·7400
1·7500	0·2000	0·0330	1·9100	0·4400	-0·3100
1·0000	-1·0000	-0·5950	1·8500	-1·0800	0·0150
0·7600	-2·1000	0·4727	0·5700	-1·7400	-0·5250
-0·7600	-2·1000	0·4727	-0·5700	-1·7400	0·5250
-1·0000	-1·0000	-0·5950	-1·8500	-1·0800	-0·0150
-1·7500	0·2000	0·0330	-1·9100	0·4400	0·3100
-1·3200	1·6500	-0·2180	-1·1200	1·3000	-0·7400
CB			**TCB**		
-0·7770	0·3482	1·5127	0·0000	2·0100	-0·0195
-0·7542	-0·9407	2·3752	1·0102	1·1410	0·8580
0·5605	-1·2212	3·1480	2·0917	0·4678	0·0200
1·4280	-2·3923	2·6185	1·6271	-0·8175	-0·7075
0·8652	-3·1581	1·3927	0·7544	-1·7920	0·1589
1·2834	-2·6186	0·0000	-0·7544	-1·7920	-0·1589
2·2336	-1·3927	0·0000	-1·6271	-0·8175	0·7075
1·5510	0·0000	0·0000	-2·0917	0·4678	-0·0200
0·0000	0·0000	0·0000	-1·0102	1·1418	-0·8585

Table 2 (cont.)

x	y	z	x	y	z
BB			**TBB**		
-0·6744	-1·2927	0·2740	-0·0000	1·6838	0·0228
-0·1576	-2·5181	-0·5242	0·7621	0·7805	-0·9815
-0·4334	-2·5043	-2·0504	2·0872	0·3038	-0·3315
0·3143	-1·4200	-2·8694	1·7631	-0·7052	0·8009
1·8361	-1·2895	-2·5999	0·2556	-1·0658	0·6400
2·3840	-2·0792	-1·3827	-0·2036	-1·0949	-0·6400
2·2336	-1·3927	0·0000	-1·7289	-0·8213	-0·8017
1·5510	0·0000	0·0000	-2·1144	0·1727	0·3248
0·0000	0·0000	0·0000	-0·8210	0·7464	0·9602
B			**TB**		
-0·5496	-1·0963	-0·9336	-0·0000	1·9849	0·0012
-1·4920	-2·0743	-0·1847	1·0246	1·1369	-0·8169
-0·9944	-3·5411	-0·2651	2·0461	0·5139	0·1060
0·5502	-3·6398	-0·1646	1·9295	-1·0317	0·2960
1·2447	-3·3182	-1·5136	0·5142	-1·4520	0·4770
2·1488	-2·0614	-1·4197	-0·4440	-1·4800	-0·4770
2·1348	-1·4369	0·0000	-1·8809	-1·1420	-0·2960
1·5510	0·0000	0·0000	-2·0868	0·3942	-0·1060
0·0000	0·0000	0·0000	-1·1030	1·0757	0·8160
C			**TC**		
-0·5618	-1·2198	0·6999	-0·0000	2·0625	0·0094
-1·4932	-2·0784	-0·1951	1·1409	1·2606	0·6882
-0·9896	-3·5392	-0·3295	2·1213	0·4814	-0·2267
0·5532	-3·6386	-0·2046	1·8944	-1·0433	-0·3980
1·2694	-3·3081	-1·5401	0·7006	-1·6863	0·3550
2·1717	-2·0520	-1·4233	-0·6797	-1·6977	-0·3524
2·1348	-1·4369	0·0000	-1·8827	-1·0695	0·3985
1·5510	0·0000	0·0000	-2·1319	0·4511	0·2219
0·0000	0·0000	0·0000	-1·1629	1·2413	-0·6958

exclude arrangements with interpenetrating non-bonded atoms. Pairs of forms, with C_2 and C_s symmetry, having the same ratio of the puckering amplitudes, formally constitute pseudorotational pathways (Boessenkool & Boeyens, 1980; Evans & Boeyens, 1988). It is noted that in the cycloalkanes, where the C_s forms are of high energy, these pathways are not low-energy interconversion modes and hence are not pseudorotational cycles in the sense described by Dale (1973b). The proposed classical nomenclature of the C_s forms is derived from the shapes of the forms in projection. Their pseudorotational partners are described as twist forms. Torsion angles of the classical forms are given in Table 1 and the forms are illustrated in Fig. 1. Cartesian coordinates are given in Table 2.

There are six Cremer & Pople (1975) puckering parameters for a nine-membered ring – three amplitude and phase-angle pairs (q_m, φ_m); $m = 2, 3, 4$. The puckering amplitudes of the classical forms are given in Table 2. As noted for eight-membered rings (Evans & Boeyens, 1988), when $q_m = 0$, φ_m has no meaning. The geometrical interpretation of the six parameters is shown in Fig. 2.

This definition may be interpreted as mapping the forms onto:

(a) A series of tori lying at positions determined by q_2 and φ_2 on a major torus.

(b) A tube, helically coiled about a torus defined by q_2, φ_2, q_4 and φ_4. q_3 and φ_3 define a point on this tube.

The former interpretation is the logical extension of the eight-membered rings mapped onto series of tori located on a sphere, whereas the latter interpretation has the advantage of mapping the forms onto a continuous tube, shown in Fig. 3.

A two-dimensional projection of either surface is achieved by projecting all forms onto $\varphi_2 = 0$. The forms then map onto a torus given by q_3, q_4, φ_3 and φ_4. A polar projection of this composite torus at $\varphi_2 = 0$, with the radial axis along the $\varphi_3 = 0$ circle, is shown in Fig. 4. Pseudorotational cycles appear as spirals. In three dimensions these may be visualized as helices on a minor torus stretched around the major torus, or as a helix wound around a tube, coiled in space. Overlap of the forms occurs at all positions S, S', T and T'. The BB–TBB cycle is illustrated as the circle J–K, where φ_4 is replaced by φ_2, to avoid projection of all forms to a point. The subscripts indicate the atom through which the symmetry element passes.

Results and discussion

The TBC–BC and TBB–BB pseudorotational cycles map onto mutually perpendicular circles, and are shown in Figs. 5 and 6. The CC and TCC forms map onto the torus defined by q_3, q_4, φ_3 and φ_4. A polar projection of this surface is shown in Fig. 7. All other pseudorotational cycles map onto the complex surface and are best viewed as two-dimensional projections in Figs. 8–12. The least confusing projecton is onto the surface given by $q_4 = 0$. A projection of the resulting torus, defined by q_2, q_3, φ_2 and φ_3, is

taken at fixed amplitudes with the phases along the Cartesian axes. The angular values are denoted by the integer k of $k\pi/18$. In all these illustrations, the atomic numbering starts at the top of each polygon and proceeds clockwise. The signs of the endocyclic torsion angles are indicated. In Figs. 8–12, the form with $\varphi_4 = 0$ is indicated. The value of φ_4 increases in steps of $\pi/18$ along each pseudorotational cycle.

The angular positions of all symmetrical forms can be expressed as integral multiples of $\pi/18$. Enantiomeric forms lie at angular positions

$$\varphi'_m = \varphi_m + \pi.$$

Each classical form X is represented as Xn, where n is the number of the atom through which the symmetry element (C_s or C_2) passes. The mirror image is denoted $\overline{Xn}$, as for seven-membered rings (Boessenkool & Boeyens, 1980). The endocyclic torsion-angle change along all pseudorotational pathways takes place gradually, decreasing in positive value to negative values, often through zero. The symmetry element through an atom becomes a symmetry element through an adjacent bond when moving along any pseudorotational cycle, except in the BB–TBB cycle, where the symmetry element through an atom progresses to a symmetry element through an adjacent atom, as observed in the B–TB cycle of seven-membered rings (Boessenkool & Boeyens, 1980).

A quantitative description of an intermediate form in terms of the conformational surface is clearly not possible, but, a mixed form can be expressed as a linear combination of primitive forms (Evans &
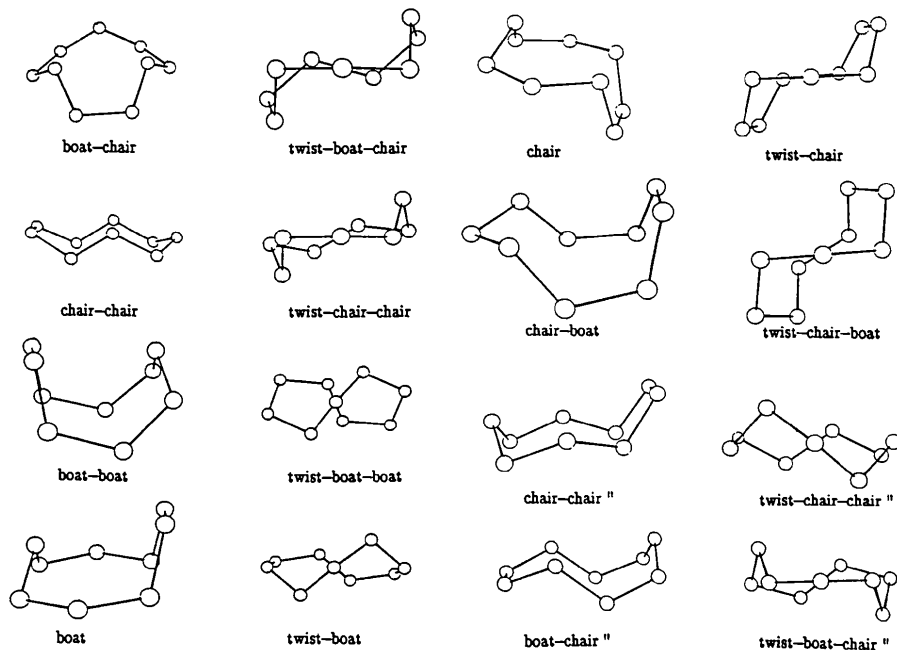

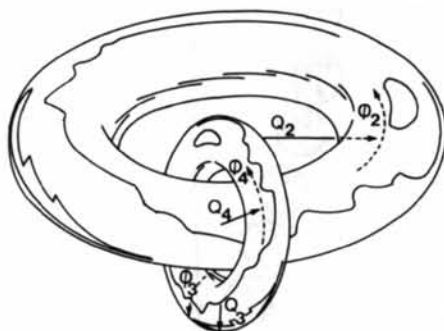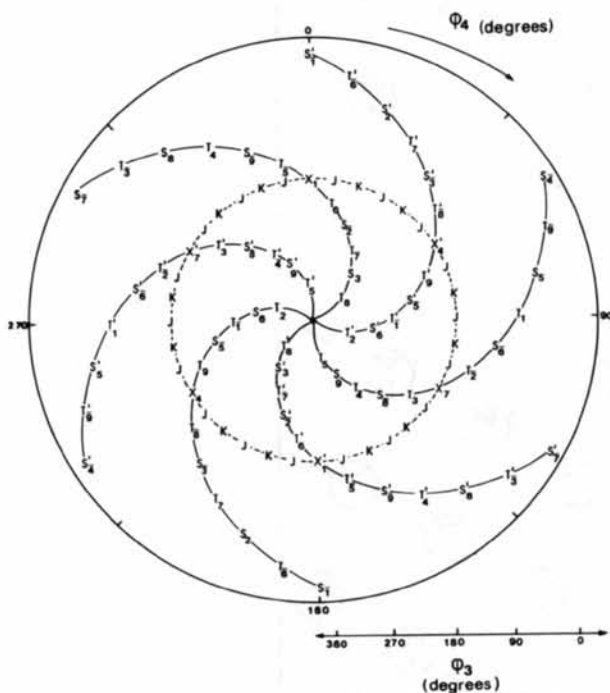Fig. 1. Symmetrical forms of nine-membered rings.

Fig. 2. Geometrical interpretation of the puckering parameters.

Fig. 3. The complex surface for the mapping of nine-membered rings.

Boeyens, 1989). Any nine-membered ring is a linear combination of the six primitive forms, illustrated in Fig. 13. The E_4 representations do not correspond with any classical forms. These primitive forms require bond lengths significantly different from those of common chemical rings. The remaining 12 classical forms are linear combinations of the six basis forms in specific relative proportions. An identification procedure to establish these forms, based on the values of their linear coefficients and phase angles, has been included as a subroutine of the program *CONFOR* (Evans & Boeyens, to be published). The description of the classical forms as linear combinations on the primitive basis is included in Table 5. The relative contributions from each E_m'' representation, and hence the shape of the puckered ring, depend only on the ratios of the q_m values. The
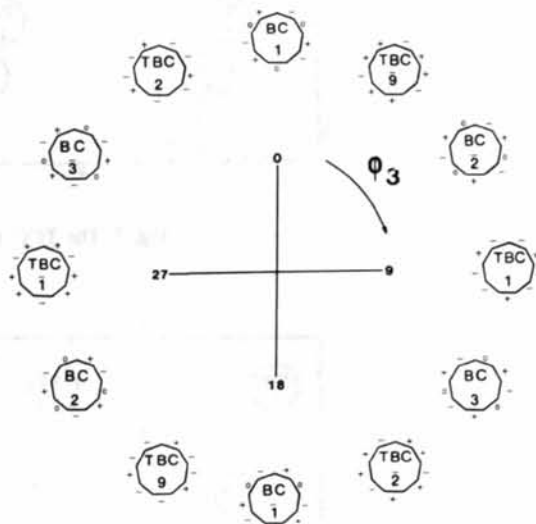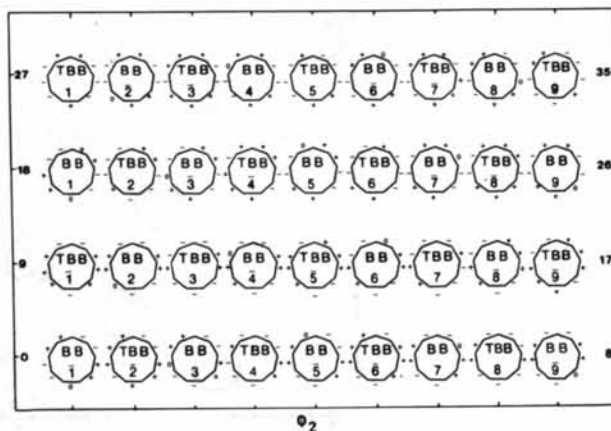

Fig. 5. The TBC–BC pseudorotational cycle.

Fig. 4. A two-dimensional projection of the surface. S = (CC, CC″, BC″, B), S' = (CB, C), T = (TCC, TCC″, TBC″, TB), T' = (TCB, TC), K = BB, J = TBB.

Fig. 6. The TBB–BB pseudorotational cycle. The circle is represented linearly for clarity.
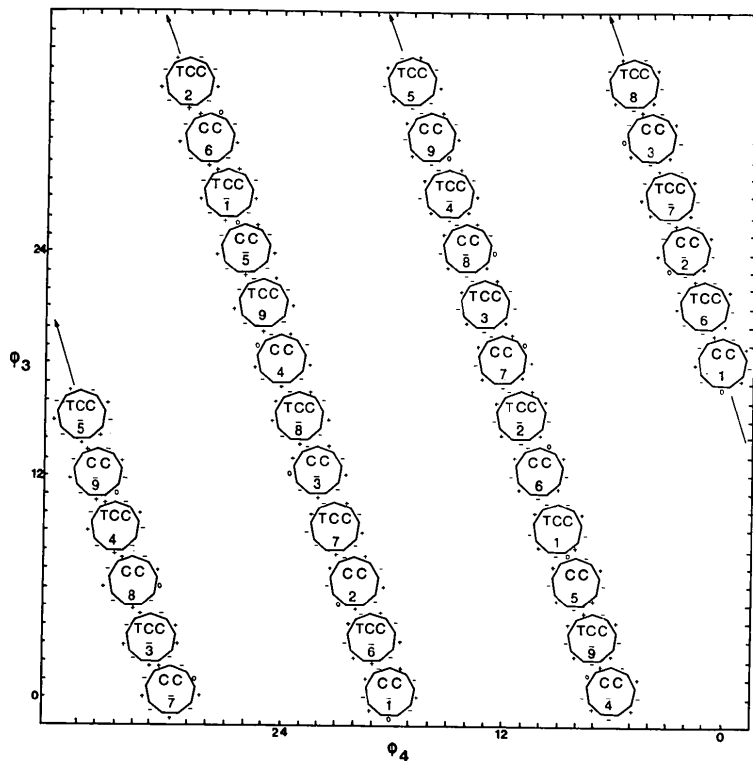
Fig. 7. The TCC–CC pseudorotational cycle.
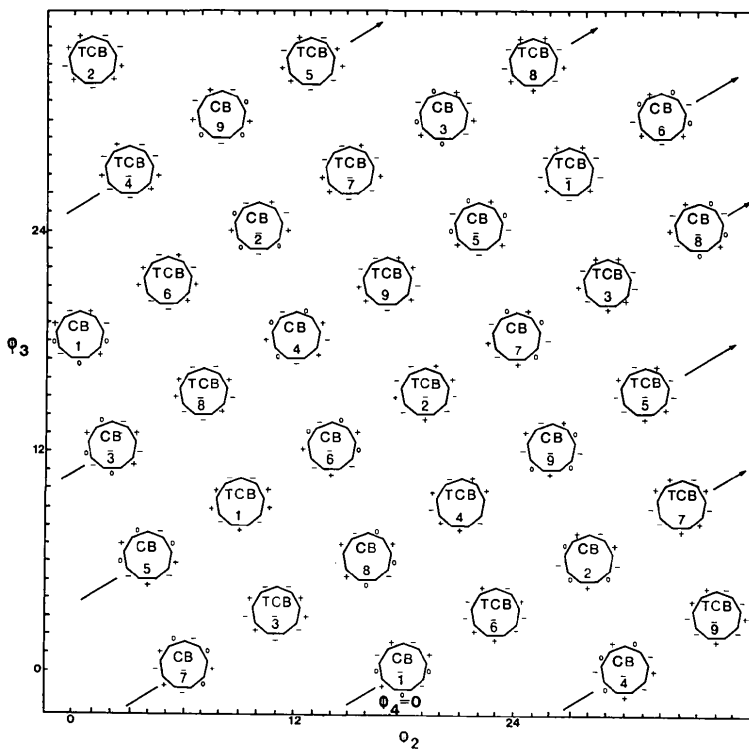
Fig. 8. The TCB–CB pseudorotational cycle.
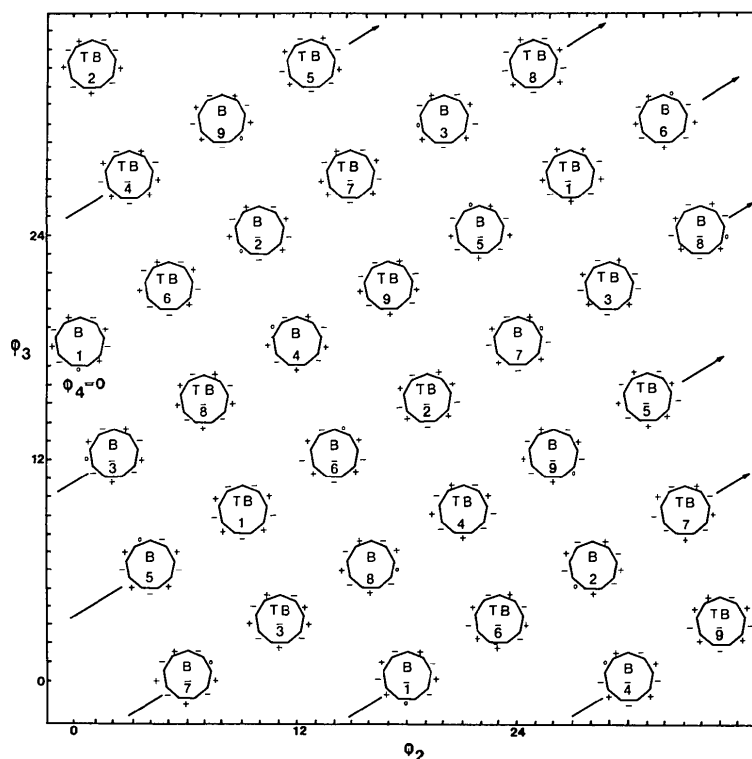
Fig. 9. The TB–B pseudorotational cycle.

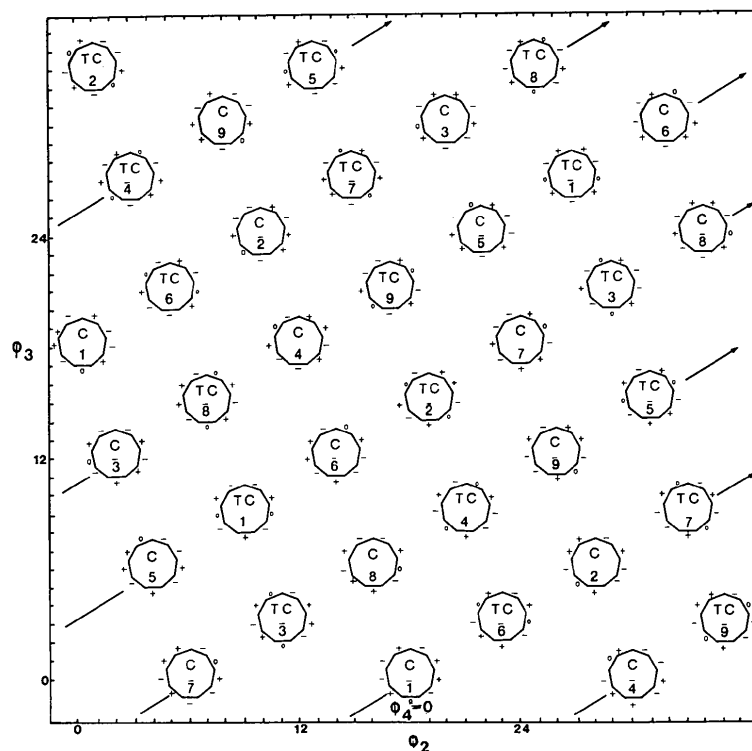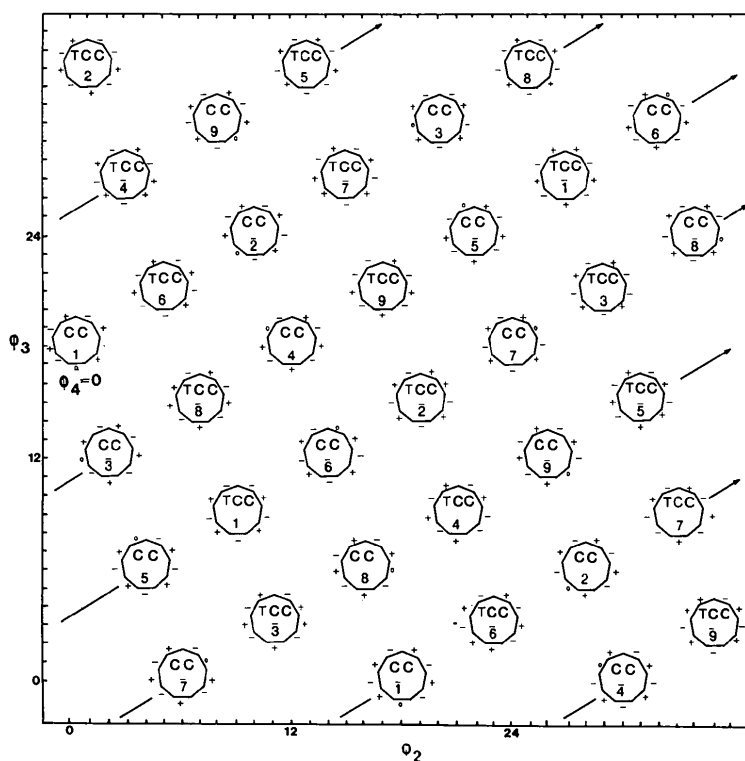Fig. 10. The TC–C pseudorotational cycle.
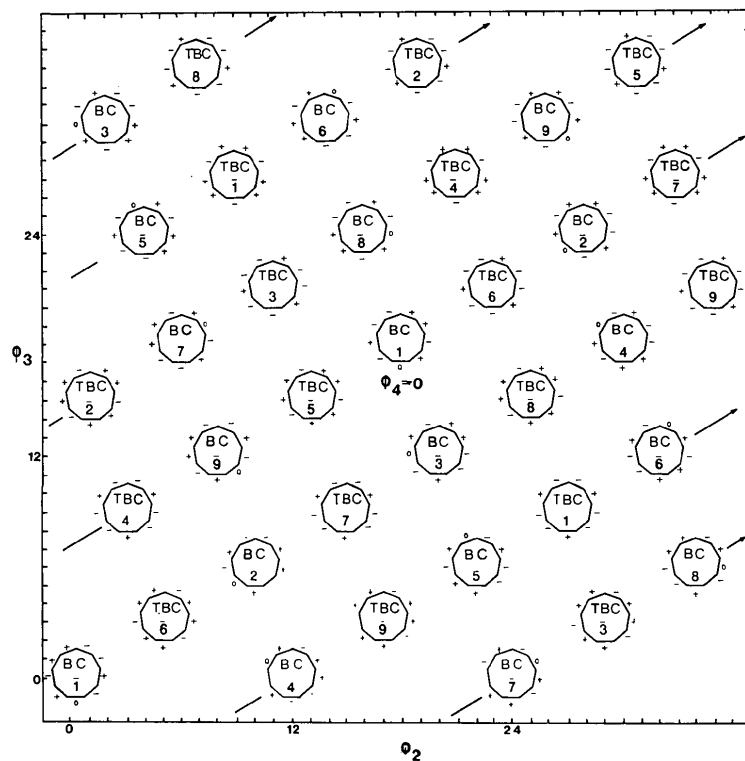
Fig. 11. The TCC″–CC″ pseudorotational cycle.

Fig. 12. The TBC″–BC″ pseudorotational cycle.

conformations of the nine-membered rings can there-fore be mapped onto a normalized surface, indepen-dent of ring type and extent of pucker, to avoid a definition of classical forms for each chemical class of rings (Petit, Dillen & Geise, 1983).

Application

Conformational analyses, reviewed by Boeyens & Dobson (1987), show that most nitrogen- and sulfur-donor macrocycles adopt either a [333] or a [234] conformation in terms of the Dale (1973a,b) formalism. The results of a puckering analysis of a number of nine-membered macrocycles, charac-terized in Fig. 14 and Table 3, are given in Table 4.

On the basis of Fig. 5, the structures (a)–(d) are described as twist–boat–chair forms with some dis-tortion to the boat–chair forms. Structures (e) and (f) cannot be correlated with any classical forms on the basis of the q_m and φ_m values. These intermediate forms are best described as a linear combination, as shown in Table 5.
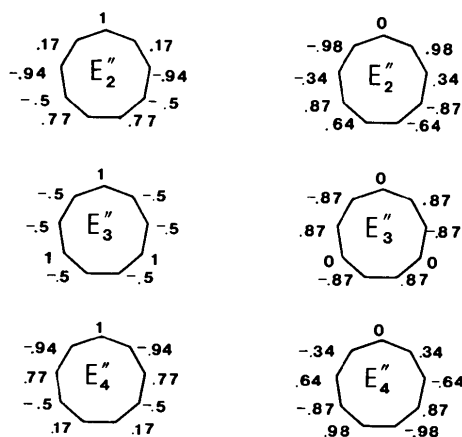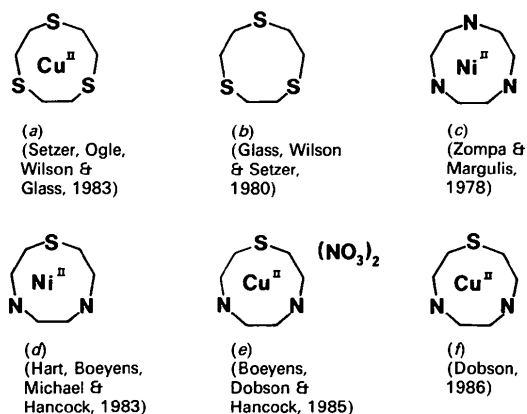

Fig. 13. Primitive forms of nine-membered rings.

Fig. 14. Nitrogen- and sulfur-donor macrocycles.

Table 3. *Endocyclic torsion angles* (°) *of nitrogen- and sulfur-donor macrocycles*

The macrocycles (a)–(f) are as defined in Fig. 14.

	(a)	(b)	(c)	(d)	(e)	(f)
ω_1	59	−131	134	−55	−116	−117
ω_2	54	58	−45	−49	50	50
ω_3	−131	55	−71	144	75	75
ω_4	59	−131	134	−74	−85	−94
ω_5	56	59	−44	−43	−44	−31
ω_6	−132	55	−70	136	150	141
ω_7	57	−131	133	−72	−67	−75
ω_8	56	59	−46	−51	−38	−36
ω_9	−132	55	−71	120	98	98

Table 4. *Puckering analysis of nitrogen- and sulfur-donor macrocycles*

Ring	q_2 (Å)	φ_2 (°)	q_3 (Å)	φ_3 (°)	q_4 (Å)	φ_4 (°)
(a)	0·01	11	1·60	157	0·01	180
(b)	0·00	18	1·59	23	0·00	46
(c)	0·02	275	1·25	206	0·01	258
(d)	0·09	337	1·36	335	0·11	352
(e)	0·60	148	1·20	354	0·38	20
(f)	0·51	156	1·20	356	0·36	16

Table 5. *The linear coefficients of some intermediate forms* [(a)–(f)] *and of the* 16 *classical conformations*

The phase angles (°) of the basis forms, denoted as k of $k\pi/18$, are given in parentheses.

	Primitive form					
	E_2''		E_3''		E_4''	
	Cos	Sin	Cos	Sin	Cos	Sin
Ring	form	form	form	form	form	form
(a)	0·00	0·00	0·25 (18)	0·75 (15)	0·00	0·00
(b)	0·00	0·00	0·22 (0)	0·78 (3)	0·00	0·00
(c)	0·00	0·00	0·13 (18)	0·86 (21)	0·00	0·00
(d)	0·04 (34)	0·02 (33)	0·15 (36)	0·73 (33)	0·01 (36)	0·05 (35)
(e)	0·05 (14)	0·23 (15)	0·44 (36)	0·11 (33)	0·17 (2)	0·00
(f)	0·14 (16)	0·11 (15)	0·51 (36)	0·07 (33)	0·10 (2)	0·07 (1)
BC	0	0	1·00	0	0	0
TBC	0	0	0	1·0	0	0
CC	0	0	0·38	0	0·62	0
TCC	0	0	0	0·38	0	0·62
C	0·28	0	0·62	0	0·10	0
TC	0	0·34	0	0·52	0	0·14
B	0·58	0	0·17	0	0·25	0
TB	0	0·58	0	0·17	0	0·25
BB	1·00	0	0	0	0	0
TBB	0	1·0	0	0	0	0
CB	0·60	0	0·25	0	0·15	0
TCB	0	0·50	0	0·32	0	0·18
BC''	0·31	0	0·56	0	0·13	0
TBC''	0	0·32	0	0·56	0	0·12
CC''	0·40	0	0·19	0	0·41	0
TCC''	0	0·40	0	0·19	0	0·41

The linear coefficients also quantify the distortion of the rings (a)–(d) from the TBC form. The results show that the conformations of rings (a)–(d) are similar, and this form can be correlated with the [333] conformation of the Dale (1973a) formalism. The 9-ane-N_3 macrocycle (ring c) shows a smaller distortion to the BC form. The 9-ane-N_2S of the Ni^{II} complex shows a slight distortion from a form on the BC–TBC cycle. The similar conformations of (e) and (f) can be correlated with the [234] conformation of the Dale (1973a) formalism.

These results corroborate previous observations (Boeyens & Dobson, 1987; Dobson, 1986): 9-ane-N$_3$, 9-ane-S$_3$ and 9-ane-N$_2$S when complexed with Ni^{II} adopt a similar conformation along the BC–TBC pseudorotational cycle. When 9-ane-N$_2$S is complexed with Cu^{II}, a different intermediate conformation is energetically preferred.

Concluding remarks

This communication completes the survey of ring conformations and the mapping of symmetrical forms on geometrical surfaces for graphical analysis of unknown configurations, from crystallographic coordinates. The procedure has been automated in the meantime and our FORTRAN program, CONFOR, which identifies the nearest symmetrical form and quantitatively defines the conformation as a linear combination of primitive forms, is available from the authors.

References

BOESSENKOOL, I. K. & BOEYENS, J. C. A. (1980). *J. Cryst. Mol. Struct.* 10, 11–18.

BOEYENS, J. C. A. (1978). *J. Cryst. Mol. Struct.* 8, 317–320.
BOEYENS, J. C. A. & DOBSON, S. M. (1987). In *Stereochemistry of Organometallic and Inorganic Compounds*, Vol. 2, edited by I. BERNAL. Amsterdam: Elsevier.
BOEYENS, J. C. A., DOBSON, S. M. & HANCOCK, R. D. (1985). *Inorg. Chem.* 24, 3073–3076.
BOEYENS, J. C. A. & EVANS, D. G. (1989). *Acta Cryst.* B45, 577–581.
CREMER, D. & POPLE, J. A. (1975). *J. Am. Chem. Soc.* 97, 1354–1358.
DALE, J. (1973a). *Acta Chem. Scand.* 27, 1115–1129.
DALE, J. (1973b). *Acta Chem. Scand.* 27, 1130–1148.
DOBSON, S. M. (1986). *A Crystallographic and Thermodynamic Study of Macrocyclic Complexes*, PhD Thesis, Univ. of the Witwatersrand, South Africa.
EVANS, D. G. & BOEYENS, J. C. A. (1988). *Acta Cryst.* B44, 663–671.
EVANS, D. G. & BOEYENS, J. C. A. (1989). *Acta Cryst.* B45, 581–590.
GLASS, R. S., WILSON, G. S. & SETZER, W. N. (1980). *J. Am. Chem. Soc.* 102, 5068–5069.
HART, S. M., BOEYENS, J. C. A., MICHAEL, J. P. & HANCOCK, R. D. (1983). *J. Chem. Soc. Dalton Trans.* pp. 1601–1606.
HENDRICKSON, J. B. (1964). *J. Am. Chem. Soc.* 86, 4854–4866.
HENDRICKSON, J. B. (1967). *J. Am. Chem. Soc.* 89, 7047–7061.
PETIT, G. H., DILLEN, J. & GEISE, H. J. (1983). *Acta Cryst.* B39, 648–651.
SETZER, W. N., OGLE, C. A., WILSON, G. S. & GLASS, R. S. (1983). *Inorg. Chem.* 22, 266–271.
ZOMPA, L. J. & MARGULIS, T. N. (1978). *Inorg. Chim. Acta*, 28, L157–159.

Electrostatic Properties of Cytosine Monohydrate from Diffraction Data

BY H.-P. WEBER* AND B. M. CRAVEN†

Crystallography Department, University of Pittsburgh, Pittsburgh, PA 15260, USA

Abstract

The charge density distribution in deuterated cytosine monohydrate [4-(^{2}H$_2$)-amino-2(1*H*)-(1-^{2}H)-pyrimidinone], C$_4$H$_2$D$_3$N$_3$O.D$_2$O, M_r = 134·15, monoclinic, $P2_1/c$, a = 7·714 (1), b = 9·825 (1), c = 7·506 (2) Å, β = 100·52 (1)°, Z = 4, has been determined from 1432 X-ray reflections [$\sin\theta/\lambda$ < 1·15 Å^{-1}, Mo $K\alpha$, λ = 0·7093 (1) Å] collected at 82 (2) K. Least-squares structure refinement assuming Stewart's rigid pseudoatom model gave $R(F)$ = 0·041, with all nuclear positions and H/D anisotropic thermal parameters having fixed values previously determined by neutron diffraction. The cytosine and water molecules are both electrically neutral within experimental error (0·09 e). Molecular dipole moments are μ = 8·0 (1·4) debye for cytosine and 2·3 (3) debye for water. For the doubly hydrogen-bonded cytosine dimer (N1—D1···N3′, N4—D4···O2′) isolated from the crystal, the electrostatic energy of interaction is estimated to be −96 (27) kJ mol^{-1}. Maps of the electrostatic potential for molecules isolated from the crystal indicate that the electronegativity of the hydrogen-bonding acceptor sites can be ranked with the water O atom, cytosine N(3) and carbonyl O(2) in decreasing order.

Introduction

The crystal structures of cytosine and its monohydrate have received considerable attention because of the importance of cytosine as a component of the

---

* Present address: Institute de Cristallographie, Université de Lausanne, BSP Dorigny, CH-1015, Lausanne, Switzerland.
† To whom correspondence should be addressed.